CONFERENCE PRE-PRINT

VALIDATED, GLOBAL EDGE-SOL TURBULENCE SIMULATIONS IN VARIOUS ELM-FREE REGIMES

W. ZHOLOBENKO*[1], K. EDER[1], K. ZHANG[1], P. ULBL[1], A. STEGMEIR[1], J. PFENNIG[1], C. PITZAL[1], A. DI SIENA[1], B. J. FREI[1], M. GRIENER[1], M. BERNERT[1], M. FAITSCH[1], F. JENKO[1], ASDEX UPGRADE TEAM[2], TCV TEAM[3], and JET CONTRIBUTORS[4]

[1]Max Planck Institute for Plasma Physics, Boltzmannstr. 2, 85748 Garching, Germany
[2]See the author list of H. Zohm *et al*, 2024 *Nucl. Fusion* **64** 112001, https://doi.org/10.1088/1741-4326/ad249d
[3]See the author list of B. P. Duval *et al*, 2024 *Nucl. Fusion* **64** 112023, https://doi.org/10.1088/1741-4326/ad8361
[4]See the author list of CF. Maggi *et al*, 2024 *Nucl. Fusion* **64** 112012, https://doi.org/10.1088/1741-4326/ad3e16,
*E-mail contact of main author: Wladimir.Zholobenko@ipp.mpg.de

Abstract

Global simulations, validated on TCV, ASDEX Upgrade and JET, are carried out to understand turbulence and transport in the edge and scrape-off layer (SOL) in conditions which are attractive for magnetic confinement fusion reactors: high-confinement, detached and without (large) ELMs. Clear differences are found between attached tokamak L-modes, type I ELMy H-modes and ELM-free regimes, in terms of driving instabilities, their saturation, flows and filaments. In particular, we have studied the enhanced D_α (EDA) and quasi-continuous exhaust (QCE) regimes, the X-point radiator (XPR) and I-mode, positive and negative triangularity, in standard and advanced divertor geometry. The impact of detachment on edge turbulence and vice versa is demonstrated. Confinement-time-long simulations are able to reproduce transitions between different regimes, and can be consistently integrated with core turbulent transport.

1 INTRODUCTION

With burning plasma experiments approaching [1, 2, 3], integrated scenarios for reactor operation must be designed to maximize the energy gain while ensuring machine durability. In particular, high-confinement operation must be integrated with a heat exhaust solution, whereby large transients such as edge-localized-modes (ELMs) are to be avoided [4]. A key uncertainty thereby is the turbulent transport [5, 6, 7] across the plasma edge and scrape-off layer (SOL). It crucially determines both the quality of confinement and the heat exhaust, but is currently among the least understood and least predictable quantities in magnetic confinement fusion devices. The GRILLIX [8, 9] and GENE-X [10, 11] codes are developed to address this challenge with predictive edge-SOL simulations.

Integrated scenarios are being researched on present tokamak experiments that combine all the requirements for a reactor [4, 12]: the improved energy confinement mode (I-mode) [13, 14], quiescent H-mode (QH-mode) [15, 16], enhanced D_α H-mode (EDA H-mode) [17], negative triangularity (NT) L-mode [18, 19, 20], the quasi-continuous exhaust (QCE) regime [21, 22] and the X-point radiator (XPR) [23, 24]. All of these regimes have H-mode-like confinement without ELMs. However, they differ in terms of accessibility, impurity accumulation, achievable densities, required shaping and compatibility with detachment. The ability to reliably quantify turbulent transport in these highly relevant scenarios will allow to further optimize the magnetic geometry and the plasma composition for best possible confinement and exhaust, and to make predictions for the next step devices.

In this manuscript, we review the progress with the GRILLIX and GENE-X codes, focusing particularly on studies of ELM-free high-confinement tokamak regimes. In section 2, the codes are introduced. In section 3, we review past and ongoing validation efforts against experiments which guide our code development. Section 4 summarizes the recent studies of ELM-free regimes. Finally, section 5 draws conclusions and provides an outlook.

2 THE GRILLIX AND GENE-X CODES

The tools employed are the drift-fluid (transcollisional) code GRILLIX [8, 9] and the gyrokinetic code GENE-X [10, 11]. Both full-f codes are based on the locally field-aligned, flux-coordinate independent (FCI) approach [25, 26], enabling efficient turbulence simulations in diverted geometry of tokamaks [27] and stellarators [28]. Both codes are electromagnetic, which is important both for the computational performance [29, 10] and for capturing correctly the turbulence [30, 9].

While the drift-fluid model in GRILLIX was originally based on the Braginskii equations [31], it now features transcollisional extensions for the parallel heat conduction and viscosity [9], including neoclassical flow damping and linear parallel Landau damping [32]. This has allowed validating the code even in H-mode conditions [9]. For a realistic plasma density source and divertor cooling, the code is coupled to a diffusive 3-moment neutral gas model [33, 34]. Together with a coronal impurity radiation model, this allows simulations in detached conditions, in particular in the X-point radiator regime [35].

The gyrokinetic code GENE-X [36] allows simulations at even lower collisionality. With the Lenard–Bernstein / Dougherty (LBD) collision operator, the code was successfully validated on the TCV tokamak [11], showing the importance of trapped electron modes (TEMs) and collisions. The TEMs are particularly important for explaining the improved confinement in negative triangularity tokamaks [37], which is not captured by GRILLIX.

While a gyrokinetic model is generally more applicable than a drift-fluid model, in particular at lower collisionality, it tends to be computationally more expensive - especially at high collisionality. Therefore, thus far, both codes have been developed in tandem in a multi-fidelity framework, with their respective domain of applicability. However, it is of course desireable to have a consistent model for arbitrary collisionalities. This was recently enabled by the spectral velocity space representation [38]. The method brings the costs of GENE-X simulations down to those of GRILLIX, keeping the high gyrokinetic fidelity, and is much less restrictive even at high collisionality. Thus, it provides a way to unify our efforts.

3 VALIDATION DRIVEN DEVELOPMENT

Any predictive model must be verified and validated [39]. Our codes were successfully validated on TCV and ASDEX Upgrade, in L- and H-mode for GRILLIX [33, 30, 34, 35, 9], negative and positive triangularity for GENE-X [10, 11, 37]. Validations are ongoing against the DIII-D and JET tokamaks, and the Wendelstein 7-AS & -X stellarators [28].

Many observables can be compared between simulations and experiments in a hierarchical fashion. At the very least, heat transport and outboard mid-plane density and (electron) temperature profiles should agree within error bars. A recent example is shown in figure 1 (left) for XPR simulations [35]. Whenever possible, ion temperature and radial electric field measurements are compared as well [9]. Naturally, also measurements in the divertor are of prime interest, including density and temperature profiles [33], heat fluxes [11, 34], but also flows [40]. In the X-point radiator regime, radiation rates from GRILLIX were compared with bolometry measurements [35], shown in figure 1 (right). Besides mean-field quantities, also turbulence characteristics can be validated. For example, in the TCV-X21 case [40], fluctuation amplitudes, skewness and kurtosis of the saturation current have been compared. More generally, even though this requires more effort, it is of high interest to compare frequency- and wavenumber-resolved fluctuation measurements and phase-shifts between them [41].

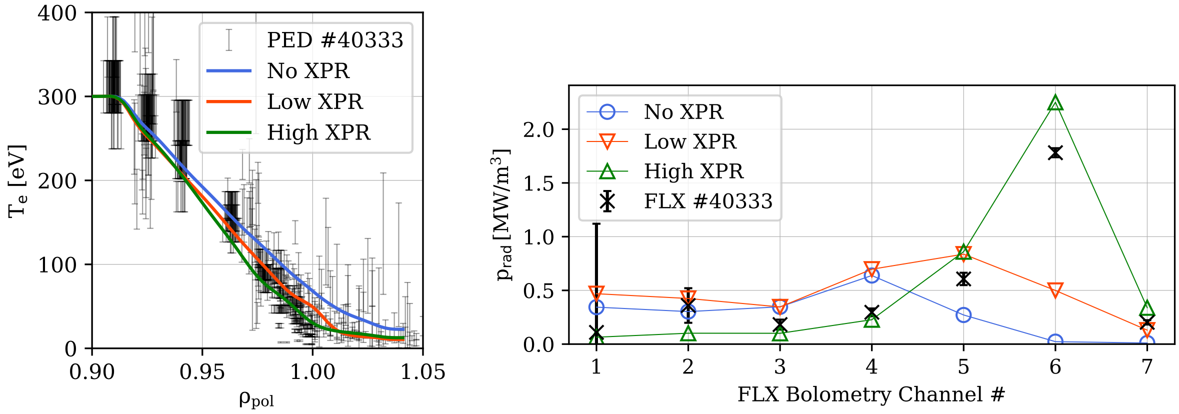

FIG. 1: Comparison of X-point radiator (XPR) GRILLIX simulations [35] and the L-mode XPR experiment #40333 on ASDEX Upgrade [24]. Colours indicate radiator height above the X-point: no XPR means attached conditions, low XPR corresponds to 5 cm, and high XPR to 12 cm. Left: OMP profiles of electron temperature compared to data from PED at 2.3 – 2.5 s. Right: Radiation compared with the bolometry system FLX at 2.38 – 2.42 s.

4 ELM-FREE REGIMES

After the successful validations, recent code applications have targeted in particular ELM-free high-confinement tokamak conditions, with the goal of explaining these and guiding the extrapolation to future reactors. These applications are discussed below. Importantly, also these simulations are carefully compared to experiments before drawing any conclusions.

4.1 Quasi-continuous exhaust

The quasi-continuous exhaust (QCE) regime has been found on ASDEX Upgrade [21, 22], in search of an ELM-free H-mode with broadened SOL heat width. Type I ELMs are avoided due to a quasi-coherent mode (QCM) at the separatrix which provides enough transport to limit the pedestal, similarly to the enhanced D_α (EDA) regime found on Alcator C-Mod [17]. But additionally, the SOL heat width is increased due to transport by blob-filaments [21]. While these can be considered as small ELMs, they are small enough to not cause any harm.

As access to QCE depends not only on high shaping, but also on a high separatrix density n_{sep} and thus collisionality, GRILLIX is perfectly suited for its investigation. The successful simulation of the QCM is shown in figure 2, which is characterized as a narrow spectrum of kinetic ballooning modes (KBMs). The QCM is more coherent and the SOL is more quiescent at low density, similarly to EDA conditions, while at high n_{sep} the QCM is less coherent and serves as a seed of blob-filaments, which increase the SOL heat width. These qualitative features were also compared in detail quantitatively with the experiment, finding excellent agreement (to be detailed in an upcoming publication).

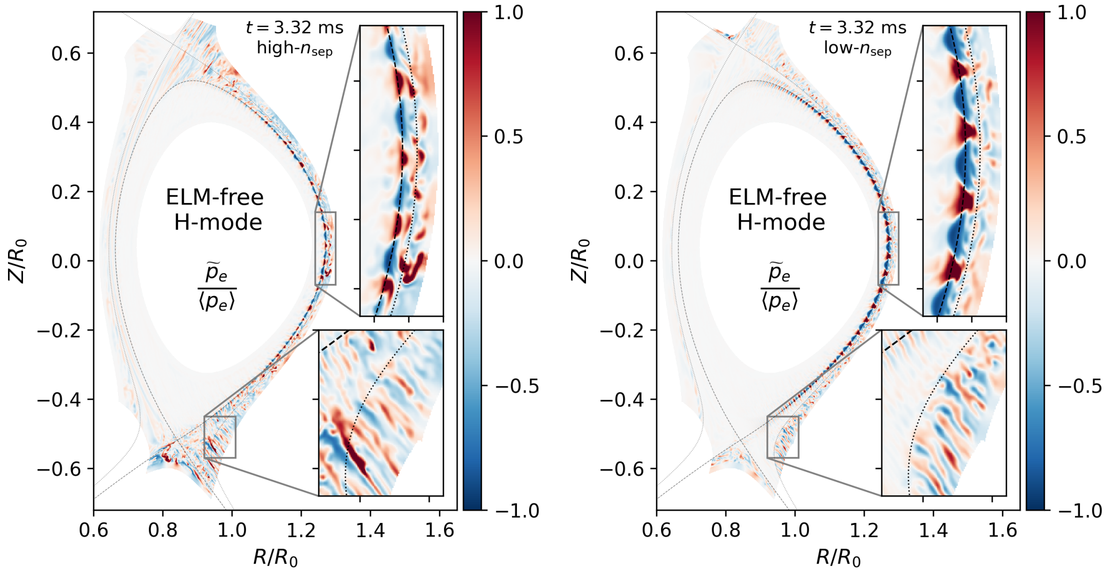

FIG. 2: Instantaneous relative fluctuations of electron pressure at a single poloidal plane for (left) the high-n_{sep} and (right) the low-n_{sep} cases in the simulation of the ELM-free H-mode discharge #36165 [21]. The black dashed line represents the separatrix, while the dotted line indicates the secondary separatrix. The color bar is truncated at $[-1, 1]$, while the actual fluctuation range extends approximately to $[-1, 3]$.

4.2 X-point radiator

Detached divertor operation is mandatory for fusion reactors to maintain acceptable heat loads and meet the material limits of the target plates [42]. In the past, full detachment, especially in carbon machines, used to be associated with unstable MARFE [43], prohibitive for operation. Nowadays, modern control techniques with seeded impurities in metal machines allow to stabilize the radiation front [44]. Additionally to featuring reduced divertor heat loads, stabilizing the radiator just a couple of centimeters above the X-point was found to reduce the pedestal by a small amount, just enough to avoid ELMs while still maintaining good H-mode confinement. Thus, the X-point radiator (XPR) offers an attractive regime of operation for a tokamak fusion reactor [24].

Access to the XPR regime can be explained with a simple 0D analytical model [23]: it requires enough cooling from neutral gas in the flux-expanded X-point volume to dissipate the parallel heat flux from upstream and allow radiative condensation, which allows to reach ideal (high) plasma density and (low) electron temperature for a seeded impurity (like nitrogen) to efficiently radiate $> 80\%$ of the input power. While the access to the XPR mostly depends on neutral gas physics, whether it becomes an unstable MARFE depends on the impurity species and is more favorable e.g. for nitrogen or neon than for carbon. More quantitative investigations have been carried out with the SOLPS code [45], showing that the XPR features a radiative mantle above the X-point where also the neutrals are ionized, while just below the mantle the temperature falls below 1 eV leading to volumetric recombination.

While SOLPS is invaluable for extrapolating XPR access to a DEMO reactor, it cannot explain the reduction of the pedestal due to the XPR (as it occurs not on the same flux surface) and ELM avoidance, and how the plasma confinement is affected. GRILLIX is able to fill in this gap, especially with its high resolution of turbulence around the X-point thanks to the FCI method [46]. We have began with L-mode XPR simulations [35]. The ionization, recombination and nitrogen radiation rates are shown in figure 3. In a time average, they compare very well to the SOLPS results [45]. However, we find that the ionization, recombination and radiation fronts are highly dynamic, moving in time. Therefore, there is no spacial separation between the fronts, they occur at the same location in the time average.

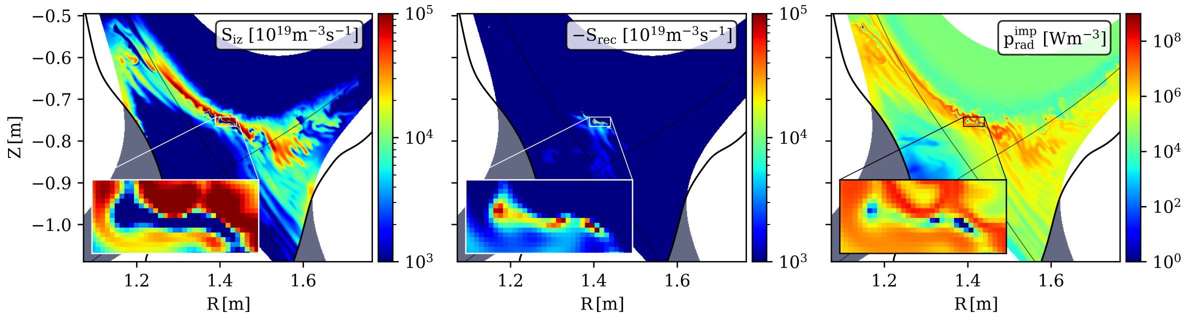

FIG. 3: Instantaneous ionization rate, recombination rate, and impurity radiation density in a simulation with an X-point radiator [35].

On the other hand, the radiative condensation together with turbulent fluctuations leads to very high fluctuation amplitudes [35]: as demonstrated in figure 4, the fluctuation statistics is highly non-Gaussian, with multiple peaks and significant skewness, and features density fluctuations with up to 500% amplitude and temperature fluctuations up to 300%. Naturally, this leads to significantly increased transport, with an order of magnitude higher anomalous diffusivities. Additionally, the cold and dense XPR leads to strong poloidal potential gradients, creating and $E \times B$ vortex cell around the XPR and increasing poloidal rotation. These observations might already explain qualitatively the pedestal reduction by the XPR, however quantitative simulations of H-mode XPR conditions are still ongoing.

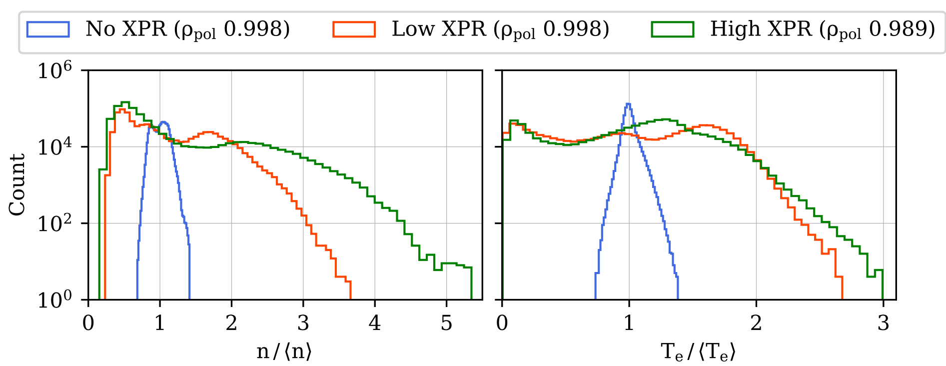

FIG. 4: Histogram of n and T_e values (normalized to their background) in the X-point radiator region [35].

Finally, due to the non-linearity of atomic reaction rates, the question arises how they are affected by such large fluctuation amplitudes [47, 48, 49]. Indeed, we find a factor 2 reduced ionization and radiation rate compared to the mean-field approximation. The recombination rate is larger by a factor 4 and much more concentrated, since temperatures < 1 eV required for atomic recombination are reached only transiently. These findings imply that mean-field simulations of detached conditions must be interpreted with care, as they miss the significant modification of reaction rates by turbulent fluctuations.

4.3 Negative triangularity

Another possibility to avoid ELMs is to avoid H-mode operation, but then, one needs to compensate for the confinement. A way to do this is with negative triangularity (NT) plasmas [18, 19, 20]: they remain in L-mode, without an edge pedestal, even at high heating and thus do not exhibit ELMs; yet, the confinement is larger than in positive triangularity (PT) L-mode plasmas by roughly a factor 2, similarly as in PT H-modes.

It is commonly believed that the confinement improvement with negative triangularity is due to trapped electron mode (TEM) turbulence [20]. Thus, it is expected to occur only at sufficiently low collisionality. While GRILLIX is better suited for high-collisionality regimes like QCE and XPR, clearly, a gyrokinetic model is required for NT vs PT studies.

Indeed, GENE-X simulations of the TCV tokamak [37], shown in figure 5, successfully recover the phenomenology: while plasma profiles remain nearly identical in NT and PT L-modes, the heat transport in NT is less than half that of PT, as shown in figure 6. Furthermore, ongoing simulations of the DIII-D tokamak confirm these findings also in high-performance operation.

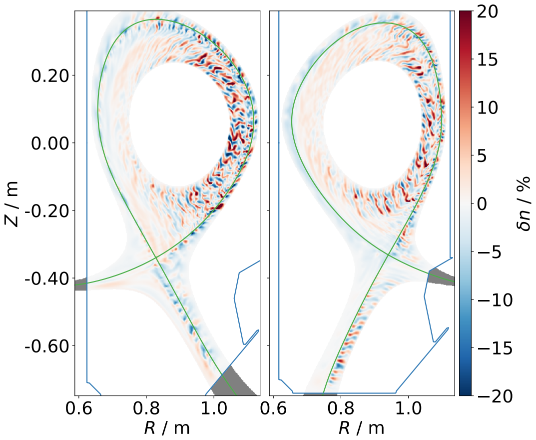

FIG. 5: Snapshots of relative density fluctuations in GENE-X simulations in positive (PT, left) and negative (NT, right) triangularity TCV [37].

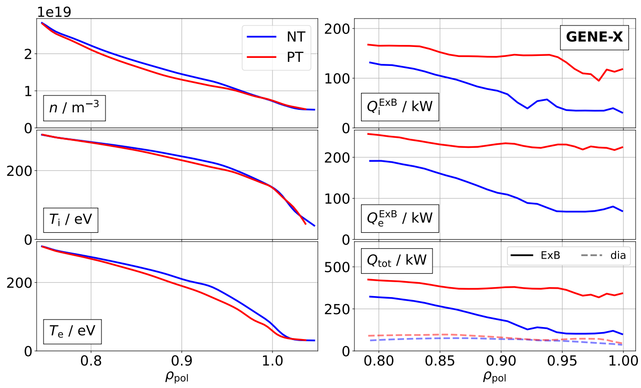

FIG. 6: OMP profiles of temporally and toroidally averaged density, ion and electron temperatures, and flux-surface integrated heat fluxes in the PT/NT TCV GENE-X simulations [37].

5 DISCUSSION, CONCLUSIONS AND OUTLOOK

We have shown that within their respective validity range, GRILLIX and GENE-X capture quantitatively key turbulence mechanisms in the tokamak plasma edge. This is demonstrated in dedicated validations in L- and H-mode, as well as in ELM-free high-performance regimes such as QCE, XPR and NT.

The high-collisionality quasi-continuous exhaust (QCE) and X-point radiator (XPR) regimes have been investigated with GRILLIX. In QCE, we reproduce the quasi-coherent mode (QCM) at the separatrix, which limits the pedestal and avoids Type-I ELMS, as well as blob-filaments seeded by the QCM which broaden the SOL width. In XPR, we find locally in the X-point region fluctuation amplitudes of up to 500% which increase transport by an order of magnitude, as well as convective cells, which might explain the ELM avoidance.

GENE-X has proven to be particularly useful in explaining differences in turbulent transport between positive and negative triangularity configurations. As trapped electron modes (TEMs) play a key role in this, GRILLIX in fact shows no significant difference between the two configurations.

Ongoing work concentrates on further ELM-free regimes, such as the I-mode, as well as regime transitions. A power scan from L- to H-mode conditions with GRILLIX reproduces qualitatively experimentally observed features, such as a fast transition in turbulence and transport, and different kinds of stationary and oscillating flows. Additionally, a coupling with GENE-Tango [50, 51] for the plasma core allows predictive simulations over the whole plasma radius.

A major development has been to extend the codes applicability from tokamaks also to stellarators [28]: the FCI method is naturally viable also in non-axisymmetric configurations, which allows both GRILLIX and GENE-X to apply their full functionality (e.g. in terms of model complexity) also for stellarator simulations.

Naturally, it is desirable to capture turbulence well both in high- and low-collisionality conditions. A promising solution to bridge the drift-fluid and the gyrokinetic limits is the spectral representation of the velocity space [38]. Its implementation in GENE-X shows the capability to reproduce grid-based results for only a fraction of the computational costs, with a speed-up of up to a factor 50, making GENE-X comparable in cost with GRILLIX. Additionally, the spectral formulation suffers much less from stiffness of the collision operator at high collisionality. Therefore, the method provides a promising way for truly predictive AND affordable simulations of reactors.

Our simulations are now clearly demonstrating their capability to capture and explain experimental behavior. On current machines, this can be used to further optimize performance, e.g. by means of plasma composition or geometrical shaping. The latter includes main plasma shaping, such as in terms of elongation and triangularity, as well as divertor shaping, e.g. using advanced divertor configurations. Moving from simulations of present experiments to reactor design, not only model fidelity but also computational performance must be improved. This is achieved by continuous optimizations, in particular for graphics card (GPU) based supercomputers [52, 53]. With this, it appears that all principal obstacles for predictive turbulence simulations of fusion reactors are resolved.

Acknowledgements

This work has been carried out within the framework of the EUROfusion Consortium, funded by the European Union via the Euratom Research and Training Programme (Grant Agreement No 101052200 — EUROfusion). Views and opinions expressed are however those of the author(s) only and do not necessarily reflect those of the European Union or the European Commission. Neither the European Union nor the European Commission can be held responsible for them. The simulations were performed on the national supercomputer HPE Apollo Hawk at the High Performance Computing Center Stuttgart (HLRS) under the grant number GRILLIX/44281, the EUROfusion Marconi-Fusion system (A3) under the Project TSVV3, and the HPC system Viper at the Max Planck Computing and Data Facility (MPCDF).

REFERENCES

[1] A. J. Creely, M. J. Greenwald, S. B. Ballinger *et al.* Overview of the SPARC tokamak. *Journal of Plasma Physics*, **86** (5) (2020).

[2] A. Loarte, R. A. Pitts, T. Wauters *et al.* The new ITER baseline, research plan and open R&D issues. *Plasma Physics and Controlled Fusion*, **67** (6), 065023 (2025).

[3] J. Lion, J.-C. Anglès, L. Bonauer *et al.* Stellaris: A high-field quasi-isodynamic stellarator for a prototypical fusion power plant. *Fusion Engineering and Design*, **214**, 114868 (2025).

[4] E. Viezzer, M. Austin, M. Bernert *et al.* Prospects of core–edge integrated no-ELM and small-ELM scenarios for future fusion devices. *Nuclear Materials and Energy*, **34**, 101308 (2023).

[5] E. Doyle, W. Houlberg, Y. Kamada *et al.* Plasma confinement and transport. *Nuclear Fusion*, **47** (6), S18 (2007).

[6] X. Garbet. Introduction to turbulent transport in fusion plasmas. *Comptes Rendus Physique*, **7** (6), 573 (2006).

[7] F. Jenko. Accelerating fusion research via supercomputing. *Nature Reviews Physics*, **7** (7), 365 (2025).

[8] W. Zholobenko, T. Body, P. Manz *et al.* Electric field and turbulence in global Braginskii simulations across the ASDEX Upgrade edge and scrape-off layer. *Plasma Physics and Controlled Fusion*, **63** (3), 034001 (2021).

[9] W. Zholobenko, K. Zhang, A. Stegmeir *et al.* Tokamak edge-SOL turbulence in H-mode conditions simulated with a global, electromagnetic, transcollisional drift-fluid model. *Nuclear Fusion*, **64** (10), 106066 (2024).

[10] D. Michels, P. Ulbl, W. Zholobenko *et al.* Full-f electromagnetic gyrokinetic turbulence simulations of the edge and scrape-off layer of ASDEX Upgrade with GENE-X. *Physics of Plasmas*, **29** (3), 032307 (2022).

[11] P. Ulbl, T. Body, W. Zholobenko *et al.* Influence of collisions on the validation of global gyrokinetic simulations in the edge and scrape-off layer of TCV. *Physics of Plasmas*, **30** (5) (2023).

[12] U. Stroth, D. Aguiam, E. Alessi *et al.* Progress from ASDEX Upgrade experiments in preparing the physics basis of ITER operation and DEMO scenario development. *Nuclear Fusion*, **62** (4), 042006 (2022).

[13] D. Whyte, A. Hubbard, J. Hughes *et al.* I-mode: an H-mode energy confinement regime with L-mode particle transport in Alcator C-Mod. *Nuclear Fusion*, **50** (10), 105005 (2010).

[14] T. Happel, P. Manz, F. Ryter *et al.* The I-mode confinement regime at ASDEX Upgrade: global properties and characterization of strongly intermittent density fluctuations. *Plasma Phys. Control. Fusion*, **59** (1), 014004 (2016).

[15] K. H. Burrell, M. E. Austin, D. P. Brennan *et al.* Quiescent H-mode plasmas in the DIII-D tokamak. *Plasma Physics and Controlled Fusion*, **44** (5A), A253 (2002).

[16] D. R. Ernst, A. Bortolon, C. S. Chang *et al.* Broadening of the Divertor Heat Flux Profile in High Confinement Tokamak Fusion Plasmas with Edge Pedestals Limited by Turbulence in DIII-D. *Physical Review Letters*, **132** (23), 235102 (2024).

[17] A. E. Hubbard and et al. Characterization of the Enhanced D-alpha H-mode in Alcator C-Mod. *Physics of Plasmas*, **8** (5), 2033 (2001).

[18] Y. Camenen, A. Pochelon, R. Behn *et al.* Impact of plasma triangularity and collisionality on electron heat transport in TCV L-mode plasmas. *Nuclear Fusion*, **47** (7), 510 (2007).

[19] M. E. Austin, A. Marinoni, M. L. Walker *et al.* Achievement of Reactor-Relevant Performance in Negative Triangularity Shape in the DIII-D Tokamak. *Phys. Rev. Lett.*, **122**, 115001 (2019).

[20] A. Marinoni, O. Sauter and S. Coda. A brief history of negative triangularity tokamak plasmas. *Reviews of Modern Plasma Physics*, **5** (1) (2021).

[21] M. Faitsch, T. Eich, G. Harrer *et al.* Broadening of the power fall-off length in a high density, high confinement H-mode regime in ASDEX Upgrade. *Nuclear Materials and Energy*, **26**, 100890 (2021).

[22] G. F. Harrer, M. Faitsch, L. Radovanovic *et al.* Quasicontinuous Exhaust Scenario for a Fusion Reactor: The Renaissance of Small Edge Localized Modes. *Physical Review Letters*, **129** (16), 165001 (2022).

[23] U. Stroth, M. Bernert, D. Brida *et al.* Model for access and stability of the X-point radiator and the threshold for marfes in tokamak plasmas. *Nuclear Fusion*, **62** (7), 076008 (2022).

[24] M. Bernert, T. Bosman, T. Lunt *et al.* X-point radiation: From discovery to potential application in a future reactor. *Nuclear Materials and Energy*, **43**, 101916 (2025).

[25] A. Stegmeir, D. Coster, O. Maj *et al.* The field line map approach for simulations of magnetically confined plasmas. *Computer Physics Communications*, **198**, 139 (2016).

[26] A. Stegmeir, T. Body and W. Zholobenko. Analysis of locally-aligned and non-aligned discretisation schemes for reactor-scale tokamak edge turbulence simulations. *Computer Physics Communications*, **290**, 108801 (2023).

[27] W. Zholobenko, J. Pfennig, A. Stegmeir *et al.* Filamentary transport in global edge-SOL simulations of ASDEX Upgrade. *Nuclear Materials and Energy*, **34**, 101351 (2023).

[28] A. Stegmeir, M. E. Finkbeiner, C. Pitzal *et al.* GRILLIX as unified fluid turbulence code for tokamaks and stellarators. *Computer Physics Communications*, **318**, 109874 (2026).

[29] A. Stegmeir, A. Ross, T. Body *et al.* Global turbulence simulations of the tokamak edge region with GRILLIX. *Physics of Plasmas*, **26** (5), 052517 (2019).

[30] K. Zhang, W. Zholobenko, A. Stegmeir *et al.* Magnetic flutter effect on validated edge turbulence simulations. *Nuclear Fusion*, **64** (3), 036016 (2024).

[31] S. I. Braginskii. Transport Processes in a Plasma. In A. M. A. Leontovich, editor, *Reviews of Plasma Physics*, volume 1. Consultants Bureau (1965).

[32] C. Pitzal, A. Stegmeir, W. Zholobenko *et al.* Landau-fluid simulations of edge-SOL turbulence with GRILLIX. *Submitted to Physics of Plasmas* (2023).

[33] W. Zholobenko, A. Stegmeir, M. Griener *et al.* The role of neutral gas in validated global edge turbulence simulations. *Nuclear Fusion*, **61** (11), 116015 (2021).

[34] K. Eder, A. Stegmeir, W. Zholobenko *et al.* Self-consistent plasma-neutrals fluid modeling of edge and scrape-off layer turbulence in diverted tokamaks. *Plasma Physics and Controlled Fusion* (2025).

[35] K. Eder, W. Zholobenko, A. Stegmeir *et al.* Simulating X-point radiator turbulence. *Nuclear Fusion*, **65** (9), 096029 (2025).

[36] D. Michels, A. Stegmeir, P. Ulbl *et al.* GENE-X: A full-f gyrokinetic turbulence code based on the flux-coordinate independent approach. *Computer Physics Communications*, **264**, 107986 (2021).

[37] P. Ulbl, A. Stegmeir, D. Told *et al.* Simulations of edge and SOL turbulence in diverted negative and positive triangularity plasmas. *Nuclear Fusion*, **65** (10), 106004 (2025).

[38] B. Frei, P. Ulbl, J. Trilaksono *et al.* Spectrally accelerated edge and scrape-off layer gyrokinetic turbulence simulations. *Computer Physics Communications*, **316**, 109817 (2025).

[39] M. Greenwald. Verification and validation for magnetic fusion. *Physics of Plasmas*, **17** (5) (2010).

[40] D. Oliveira, T. Body, D. Galassi *et al.* Validation of edge turbulence codes against the TCV-X21 diverted L-mode reference case. *Nuclear Fusion*, **62** (9), 096001 (2022).

[41] K. Höfler, T. Görler, T. Happel *et al.* Milestone in predicting core plasma turbulence: successful multi-channel validation of the gyrokinetic code GENE. *Nature Communications*, **16** (1) (2025).

[42] R. Pitts, X. Bonnin, F. Escourbiac *et al.* Physics basis for the first ITER tungsten divertor. *Nuclear Materials and Energy*, **20**, 100696 (2019).

[43] B. Lipschultz, B. LaBombard, E. Marmar *et al.* Marfe: an edge plasma phenomenon. *Nuclear Fusion*, **24** (8), 977 (1984).

[44] M. Bernert, F. Janky, B. Sieglin *et al.* X-point radiation, its control and an ELM suppressed radiating regime at the ASDEX Upgrade tokamak. *Nuclear Fusion*, **61** (2), 024001 (2020).

[45] O. Pan, M. Bernert, T. Lunt *et al.* SOLPS-ITER simulations of an X-point radiator in the ASDEX Upgrade tokamak. *Nuclear Fusion*, **63** (1), 016001 (2022).

[46] A. Stegmeir, D. Coster, A. Ross *et al.* GRILLIX: a 3D turbulence code based on the flux-coordinate independent approach. *Plasma Physics and Controlled Fusion*, **16** (3), 035005 (2018).

[47] Y. Marandet, A. Mekkaoui, D. Reiter *et al.* Effects of turbulent fluctuations with prescribed statistics on passive neutral particle transport in plasmas. *Plasma physics and controlled fusion*, **53** (6), 065001 (2011).

[48] D. Fan, Y. Marandet, P. Tamain *et al.* Effect of turbulent fluctuations on neutral particles transport with the TOKAM3X-EIRENE turbulence code. *Nuclear Materials and Energy*, **18**, 105 (2019).

[49] M. V. Umansky, B. I. Cohen and I. Joseph. Simulations of tokamak edge plasma turbulent fluctuations based on a minimal 3D model. *Plasma Physics and Controlled Fusion*, **66** (4), 045015 (2024).

[50] J. B. Parker, L. L. LoDestro, D. Told *et al.* Bringing global gyrokinetic turbulence simulations to the transport timescale using a multiscale approach. *Nuclear Fusion*, **58** (5), 054004 (2018).

[51] A. Di Siena, A. Bañón Navarro, T. Luda *et al.* Global gyrokinetic simulations of ASDEX Upgrade up to the transport timescale with GENE–Tango. *Nuclear Fusion*, **62** (10), 106025 (2022).

[52] A. Stegmeir, C. Lalescu, M. Lin *et al.* A high-performance elliptic solver for plasma boundary turbulence codes (2025).

[53] J. Trilaksono, P. Ulbl, J. Williams *et al.* OpenACC and OpenMP-Accelerated Fortran/C++ Gyrokinetic Fusion Code GENE-X for Heterogeneous Architectures. In *Proceedings of the Platform for Advanced Scientific Computing Conference*, PASC '25, pages 1–12. ACM (2025).